RSC Advances

PAPER

View Article Online
View Journal | View Issue

Cite this: *RSC Adv.*, 2018, **8**, 7514

Detection of cofilin mRNA by hybridization-sensitive double-stranded fluorescent probes†

Ha Jung Lee, Gui Han Go, Jong Jin Ro and Byeang Hyean Kim *

Received 15th December 2017
Accepted 10th February 2018

DOI: 10.1039/c7ra13349a

rsc.li/rsc-advances

We have developed hybridization-sensitive fluorescent oligonucleotide probes that, in the presence of quencher strands, undergo efficient fluorescence quenching through the formation of partial DNA/DNA duplexes. In the presence of target RNA, rapid displacement of the quencher strands results in highly enhanced fluorescence.

The detection of biomolecules is an important part of any investigation into their biological mechanisms and phenomena. Fluorescence-based methods are particularly useful for providing interpretable signals for various targets (*e.g.*, genes, proteins, small molecules). When nucleic acids are used as probes, they can provide sequence-specific information regarding the binding (through hydrogen bonding) of target nucleic acids. Because of their high sequence-specificity, many fluorescent hybridization probes, including molecular beacons (MBs), have been developed and applied for nucleic acid detection and visualization.[1,2]

In previous studies, we found that a quencher-free molecular beacon (QF-MB) containing the pyrene-modified nucleoside ^{Py}U exhibited a high fluorescence enhancement in the presence of trinucleotide repeats, especially for RNA.[3,4] Among various fluorescent nucleobase derivatives, uracil derivatives have been particularly useful for selective detection of specific sequences, taking advantage of changes in photoinduced electron transfer between the fluorophore and the neighboring base.[3–5] To apply such systems to various other target sequences, here we designed fully complementary sequences and incorporated the internal fluorescent nucleoside ^{Py}U in place of a thymine residue, resulting in a significantly increased fluorescence signal based on strand displacement (Fig. 1). Incorporation of a ^{Py}U unit in a single strand of the probe sequence and hybridization with a strand partially complementary to the probe strand containing a pyrene unit as a fluorescence quencher can lead to improved discrimination factors.[4,6] Such partially double-stranded probes have several attractive features.

First, the probe sequence does not require an additional sequence in its strand that is not complementary to the target sequence to ensure formation of a secondary structure (*e.g.*, a hairpin). Such additional sequences might interfere with the specific hybridization between the probe and the target sequence. Accordingly, double-stranded fluorescence probes should allow the specific detection of many kinds of targets. Second, the highly quenched initial fluorescence signal, due to the formation of a partial duplex, results in significantly increased fluorescence in the presence of the target; the incorporation of a hybridization-sensitive internal fluorophore provides a stable and sensitive fluorescence signal upon perfect hybridization with the target.

Cofilin is a protein that regulates the activity of actin, which is related to the formation of the cytoskeleton in cells. Actin plays a crucial role in the growth and elongation of cells,[7] especially in neurons and, therefore, in the control of neurotransmission. We designed probe strands complementary to the 3′-untranslated region (3′-UTR) of target cofilin mRNA and synthesized three kinds of 19-*mer* probe strands (**P1–P3**) containing one or two ^{Py}U units in each strand (Table 1). We measured the absorption and fluorescence emission spectra of these probes as both single strands and as double strands with

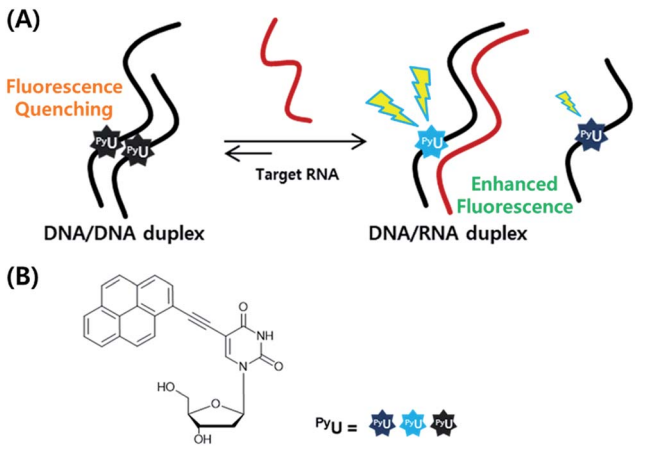

Fig. 1 (A) Schematic representation of the strand displacement process developed in this present system. (B) Structures of the internal fluorophore ^{Py}U.

Department of Chemistry, Division of Advanced Materials Science, Pohang University of Science and Technology (POSTECH), Pohang 37673, Republic of Korea. E-mail: bhkim@postech.ac.kr

† Electronic supplementary information (ESI) available. See DOI: 10.1039/c7ra13349a

Table 1 Oligonucleotide sequences of probe and target strands

Name	Sequence
P1	5′-GGT GCC ^{Py}UAG GAC GGG ACT T-3′
P2	5′-GGT GCC TAG GAC GGG AC^{Py}U T-3′
P3	5′-GGT GCC ^{Py}UAG GAC GGG AC^{Py}U T-3′
U5	3′-CA CGG ^{Py}UTC CTG-5′
U6	3′-CCA CGG ^{Py}UTC CTG C-5′
T19[a]	5′-a agu ccc guc cua ggc acc-3′
T19-U[a,b]	5′-a agu ccc guc cu*u* ggc acc-3′
T19-G[a,b]	5′-a agu ccc guc cu*g* ggc acc-3′
T19-C[a,b]	5′-a agu ccc guc cu*c* ggc acc-3′

[a] Target RNA sequence. [b] Underlined letter indicates a single mismatched base.

target RNA (Fig. 2A and S1, ESI†). The fluorescence intensities of **P1** and **P3** increased dramatically after binding with the target RNA **T19**—by 17.6- and 16.0-fold, respectively. For the probe **P2** (in which the ^{Py}U residue was located close to the 3′-end), however, the fluorescence enhancement was very low: only 1.8-fold (Table S2, ESI†). We assume that terminal modification of the ^{Py}U unit in the probe resulted in weak base pairs around the ^{Py}U residue than did central modification, resulting in a decrease in fluorescence enhancement (Table S3, ESI†).[8] Because flanking base pairs around the ^{Py}U unit are relatively less rigid compared to central base pairs, the microenvironment of ^{Py}U in the duplex formed from **P2** and **T19** is different from the central modification. Therefore, the fluorescence intensity did not increase significantly compared to the single-stranded **P2**. The absorption spectrum of **P2** in the presence of **T19** exhibited a relatively less intense absorption band than that of the duplex formed from **P1** and **T19**—the latter featured an intense signal corresponding to the high fluorescence intensity (Fig. S1, ESI†).[9,10] Even though two ^{Py}U units were incorporated into the single strand **P3**, its fluorescence enhancement was similar to that of probe **P1** containing only one ^{Py}U unit. Among other examined probe sequences complementary to other parts of 3′-UTR in cofilin mRNA, **P6** (containing two ^{Py}U units) also exhibited fluorescence intensity similar to those of **P4** and **P5**, single-^{Py}U – containing probes each modified in the central position (Fig. S2, ESI†). These results suggest that single modification of a ^{Py}U unit in the probe sequence is more efficient than dual modification, in terms of inducing high fluorescence enhancement with target RNA.

Next, to improve the fluorescence enhancement in the presence of the target, the background signal of the probe was decreased by mixing it with a pyrene-modified short oligonucleotide, a so-called "quencher strand", capable of quenching the fluorescence of the ^{Py}U unit. Two pyrene units on the opposite side in the duplex resulted in fluorescence quenching because pyrene moieties are stacked each other and located in a highly polar environment.[4,9] Such duplexes containing probe and quencher strands would have to undergo displacement of the quencher strand prior to hybridization of the target strand. First, we tested the effects of a ^{Py}U residue located in the quencher strand at the central position, opposite the ^{Py}U residue in the probe strand, potentially minimizing the fluorescence of the ^{Py}U residue in the probe strand through π-stacking of the two pyrene units in the duplex.[4,11] We synthesized the quencher strands **U5** and **U6**, each containing a ^{Py}U residue, and examined the relationship between the quenching efficiency and stable hybridization of the probe/quencher duplexes upon varying the length of the quencher strand (Table 1). The fluorescence intensity of the probe was indeed affected by the length of the quencher strand (Fig. 2B). The more stable the partial duplex is formed, the more effective stacking interaction between pyrene moieties close to each other can be possible.[12] In the presence of the ^{Py}U-modified quencher strands, the quenching efficiency of the probe at 435 nm was 65% for **U5** and 80% for **U6**. As a result, the enhancements in fluorescence for the probe in the presence of the target **T19** were 51.5- and 66.7-fold for **U5** and **U6**, respectively (Fig. 2C and S7, ESI†) much higher than that for **P1** alone. Notably, these fluorescence signals were generated not only from the probe/target duplexes but also from the released quencher strands (*i.e.*, the single-stranded quencher strands also exhibited fluorescence to some degree). Therefore, the actual fluorescence signal arising from hybridization of the probe with the target was slightly lower than that observed in the fluorescence spectra; we estimated that the additional

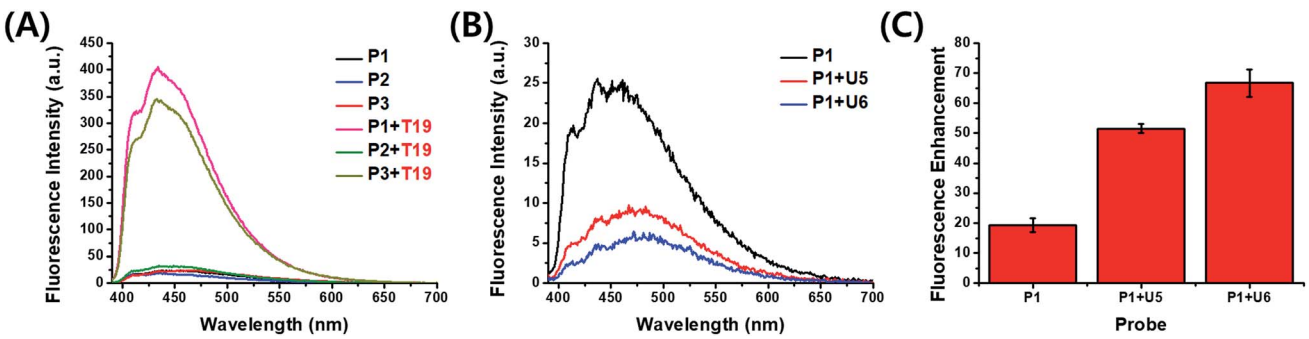

Fig. 2 (A, B) Fluorescence emission spectra of (A) the probes **P1**–**P3** with **T19** and (B) the probe **P1** with **U5** and **U6**. (C) Fluorescence enhancements (F/F_0) at 432 nm of **P1** in the presence of **U5** and **U6** upon binding with **T19**; 1.0 μM of samples in 100 mM Tris-HCl buffer (pH 7.2), 100 mM NaCl and 10 mM $MgCl_2$; annealing: 90 °C; excitation wavelength: 380 nm; excitation/emission slit: 5 nm/5 nm; F: fluorescence intensity at 432 nm of the probe **P1** with the target RNA **T19** in the absence or presence of a quencher strand **U5** and **U6**; F_0: fluorescence intensity at 432 nm of the probe **P1** in the absence or presence of a quencher strand **U5** and **U6**.

signals due to the release of **U5** and **U6** increased the fluorescence intensity by 7% (Fig. S7, ESI†). In other words, the released quencher strands added to the fluorescence enhancement of the DNA/RNA duplex. Moreover, we also tested the effect of incorporating a dabcyl derivative, ^{Dab}U, as a typical fluorescence quencher on the quencher strand and compared its effects with those of the quencher strand containing a ^{Py}U unit (Table S4, Fig. S4, ESI†). The ^{Py}U-modified quencher strands provided the probe with similar quenching in fluorescence as did ^{Dab}U-modified quencher strands of the same length (Fig. S8 and S9, ESI†). The melting temperatures (Fig. S10, Table S5, ESI†) of the duplexes of the ^{Py}U-modified quencher strands and **P1** (for **U5** and **U6** with **P1**: 60.1 and 66.0 °C, respectively) were higher than those of the natural strands and **P1** (for **N5** and **N6** with **P1**: 46.8 and 56.0 °C, respectively); the former were stabilized through π-stacking of the ^{Py}U units (Fig. S5 and S6, ESI†). The formation of duplexes from the probe and quencher strands was evident also in circular dichroism (CD) and polyacrylamide gel electrophoresis (PAGE) experiments (Fig. S11 and S12, ESI†).

To confirm the effective strand displacement of the quencher strand from the probe strand, we conducted time-dependent fluorescence experiments after addition of the target RNA **T19** to probe/quencher duplexes (Fig. 3). After addition of the target strand to the single strand of **P1**, hybridization was complete within 30 min (*i.e.*, the increase in fluorescence at 435 nm was minor thereafter). In contrast, the fluorescence intensity of **P1** in the presence of the 11-*mer* quencher strand **U5** was relatively rapid, reaching equilibrium after 20 min; for the 13-*mer* strand **U6**, however, equilibrium was reached within 35 min. Thus, compared with the single-stranded probe **P1**, the hybrid of **P1** with **U5** reacted more rapidly with the target **T19**, but the reaction time of the hybrid of **P1** with **U6** responding to the target **T19** was slightly slower than that of **P1** in the absence of a quencher strand. We suspect that the probe strand in the absence of a quencher strand was stabilized by stacking of the nucleobases; the probe would take some time to hybridize with the target RNA, requiring unfolding of its stacked bases. For the partially hybridized duplexes, however, the non-bonded sequence of the probe would be exposed, facilitating hybridization with the target strand. As a result, the response of **P1** in the presence of **U5** toward the target RNA was slightly faster than that of single-stranded **P1** alone. Thus, as the length of the non-bonding sequence of **P1** in the partial duplex decreased by increasing the length of quencher strand, the rate of strand displacement decreased accordingly.[13–16] Indeed, the reaction time for the probe strand in the presence of the 15-*mer* strand **U7** was much longer than those in the presence of the 11- and 13-*mer* quencher strands, because only a four-nucleotide sequence was available for hybridization of the target stand **T19** (Fig. S13, ESI†); in addition, the equilibrium of the reaction shifted to the left, in conjunction with a smaller enhancement in fluorescence.

We also tested the selectivity of the probe **P1** itself against single-base-mismatched target RNA (Fig. 4, Table 1). Target RNA strands with mismatched bases opposite the ^{Py}U residue in the probe strand provided no enhancements in fluorescence when the mismatched bases were uracil and cytosine. When guanine was the mismatched base, however, the presence of the target RNA led to a slightly increased signal. These fluorescence spectra suggest that the probe **P1** is capable of selective fluorescence enhancements that can distinguish single-base-mismatched target RNA.

In conclusion, we have developed a double-stranded duplex that functions as a universal probe that is highly specific for the sequence of its target RNA—in this case, for cofilin mRNA. When the ^{Py}U-modified probe strand was partially hybridized with quencher strands containing a ^{Py}U unit, the fluorescence intensity decreased dramatically as a result of π-stacking of the ^{Py}U units. The probe/quencher hybrids provided even greater fluorescence enhancements after stable binding of the target RNA strand with the additional signal from the released quencher strand further improving the fluorescence detection of the target RNA.

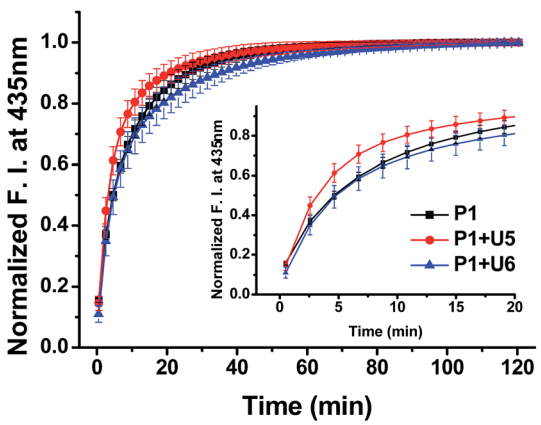

Fig. 3 Time-dependent fluorescence of **P1** in the presence of **U5** and **U6** after addition of **T19**; 1.0 μM of samples in 100 mM Tris-HCl buffer (pH 7.2), 100 mM NaCl and 10 mM $MgCl_2$; excitation wavelength: 380 nm; emission wavelength: 435 nm; excitation/emission slit: 5 nm/5 nm; temperature: 20 °C.

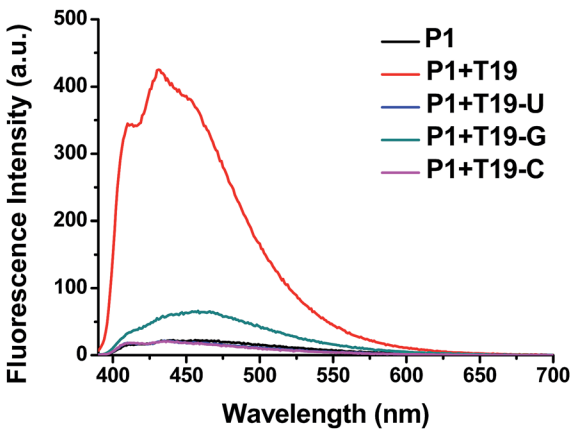

Fig. 4 Fluorescence emission spectra of **P1** in the presence of single-base-mismatched target RNA; 1.0 μM of sample in 100 mM Tris-HCl buffer (pH 7.2), 100 mM NaCl and 10 mM $MgCl_2$; annealing: 90 °C; excitation wavelength: 380 nm; excitation/emission slit: 5 nm/5 nm.

Conflicts of interest

There are no conflicts to declare.

Acknowledgements

We are grateful to the NRF of Korea (2017R1A2A1A18071086 and 2015M3A9B8029067) and thank Prof. K. T. Kim for offering sequence information used in this study.

Notes and references

1 (*a*) S. Tyagi and F. R. Kramer, *Nat. Biotechnol.*, 1996, **14**, 303; (*b*) J. Zheng, R. Yang, M. Shi, C. Wu, X. Fang, Y. Li, J. Li and W. Tan, *Chem. Soc. Rev.*, 2015, **44**, 3036; (*c*) K. Wang, Z. Tang, C. J. Yang, Y. Kim, X. Fang, W. Li, Y. Wu, C. D. Medley, Z. Cao, J. Li, P. Colon, H. Lin and W. Tan, *Angew. Chem., Int. Ed.*, 2009, **48**, 856; (*d*) A. A. Martí, S. Jockusch, N. Stevens, J. Ju and N. J. Turro, *Acc. Chem. Res.*, 2007, **40**, 402.

2 S. A. E. Marras, S. Tyagi and F. R. Kramer, *Clin. Chim. Acta*, 2006, **363**, 48.

3 N. Venkatesan, Y. J. Seo and B. H. Kim, *Chem. Soc. Rev.*, 2008, **37**, 648.

4 (*a*) K. T. Kim, R. N. Veedu, Y. J. Seo and B. H. Kim, *Chem. Commun.*, 2014, **50**, 1561; (*b*) G. T. Hwang, Y. J. Seo and B. H. Kim, *Tetrahedron Lett.*, 2005, **46**, 1475; (*c*) Y. J. Seo, G. T. Hwang and B. H. Kim, *Tetrahedron Lett.*, 2006, **47**, 4037.

5 (*a*) J. H. Ryu, J. Y. Heo, E.-K. Bang, G. T. Hwang and B. H. Kim, *Tetrahedron*, 2012, **68**, 72; (*b*) J. W. Lee, Y.-S. Son, J. Y. Hwang, Y. Park and G. T. Hwang, *Org. Biomol. Chem.*, 2017, **15**, 7165; (*c*) G. T. Hwang, Y. J. Seo and B. H. Kim, *J. Am. Chem. Soc.*, 2004, **126**, 6528.

6 M. Kovaliov, C. Wachtel, E. Yavin and B. Fischer, *Org. Biomol. Chem.*, 2014, **12**, 7844.

7 (*a*) K. Ohashi, *Dev., Growth Differ.*, 2015, **57**, 275; (*b*) Y. Maizels, F. Oberman, R. Miloslavski, N. Ginzach, M. Berman and J. K. Yisraeli, *J. Cell Sci.*, 2015, **128**, 1922; (*c*) J. R. Bamburg and B. W. Bernstein, *F1000 Biol. Rep.*, 2010, **2**, 62.

8 (*a*) A. Pasternak and J. Wengel, *Org. Biomol. Chem.*, 2011, **9**, 3591; (*b*) M. Gładysz, J. Nowak-Karnowska, A. Pasternak and J. Milecki, *Bioorg. Chem.*, 2017, **72**, 161.

9 (*a*) N. Amann, E. Pandurski, T. Fiebig and H.-A. Wagenknecht, *Chem.–Eur. J.*, 2002, **8**, 4877; (*b*) C. Boonlua, C. Vilaivan, H.-A. Wagenknecht and T. Vilaivan, *Chem.–Asian J.*, 2011, **6**, 3251; (*c*) A. Trifonov, I. Buchvarov, H.-A. Wagenknecht and T. Fiebig, *Chem. Phys. Lett.*, 2005, **409**, 277; (*d*) E. Mayer, L. Valis, C. Wagner, M. Rist, N. Amann and H.-A. Wagenknecht, *ChemBioChem*, 2004, **5**, 865; (*e*) M. Rist, N. Amann and H.-A. Wagenknecht, *Eur. J. Org. Chem.*, 2003, **13**, 2498.

10 M. Nakamura, Y. Fukunaga, K. Sasa, Y. Ohtoshi, K. Kanaori, H. Hayashi, H. Nakano and K. Yamana, *Nucleic Acids Res.*, 2005, **33**, 5887.

11 U. Förster, K. Lommel, D. Sauter, C. Grünewald, J. W. Engels and J. Wachtveitl, *ChemBioChem*, 2010, **11**, 664.

12 S. M. Langenegger and R. Häner, *Chem. Commun.*, 2004, 2792.

13 Q. Li, G. Luan, Q. Guo and J. Liang, *Nucleic Acids Res.*, 2002, **30**, e5.

14 S. Huang, J. Salituro, N. Tang, K.-C. Luk, J. J. Hackett, P. Swanson, G. Cloherty, W.-B. Mak, J. Robinson and K. Abravaya, *Nucleic Acids Res.*, 2007, **35**, e101.

15 (*a*) D. Meserve, Z. Wang, D. D. Zhang and P. K. Wong, *Analyst*, 2008, **133**, 1013; (*b*) V. Gidwani, R. Riahi, D. D. Zhang and P. K. Wong, *Analyst*, 2009, **134**, 1675; (*c*) R. Riahi, Z. Dean, T.-H. Wu, M. A. Teitell, P.-Y. Chiou, D. D. Zhang and P. K. Wong, *Analyst*, 2013, **138**, 4777.

16 S. Barrois and H.-A. Wagenknecht, *Org. Biomol. Chem.*, 2013, **11**, 3085.